Model Based Predictive Control with a Fixed Switching Frequency Applied to a Single-Phase Cascade H-Bridge Multilevel STATCOM

L. Comparatore*, J. Rodas*, M. Rivera†, R. Gregor*, J. Pacher*, A. Renault*, J. Muñoz† and P. Sanjeevikumar††

*Laboratory of Power and Control Systems, Facultad de Ingeniería, Universidad Nacional de Asunción, Paraguay

E-mail: {lcomparatore, jrodas, rgregor, jpacher, arenault}@ing.una.py

†Department of Electrical Engineering, Universidad de Talca, Chile

E-mail: {marcoriv, jmunoz}@utalca.cl

††Department Electrical and Electronics Engineering, University of Johannesburg, South Africa

E-mail: sanjeevi_12@yahoo.co.in

***Abstract*—Classical model based predictive control for single-phase cascade H-bridge multilevel STATCOM generates a variable switching frequency that produces high frequency harmonics and high stress on the power semiconductor devices. To solve these issues, in this paper is proposed a predictive control strategy operating at fixed switching frequency. The method includes a modulation stage in the predictive control algorithm. Simulation results show increased performance of the proposed control method in terms of ripple amplitude and total harmonic distortion.**

***Index Terms*—Cascade H-bridge converter, fixed switching frequency, predictive control.**

I. Introduction

Novel control strategies and its applications in the field of the power electronic converters are mainly due to the achieved development in power semiconductor devices as well as the fast growth of digital signal processors capacity processing [1]. Model based predictive control (MBPC) has recently gained the attention of the scientific community like a real alternative for controlling power converters, mainly due to some specific advantages such as: flexibility, fast transient response and its simplicity for incorporating restrictions and constraints, since it is possible to represent the different control objectives by using a defined cost function [1]. Nevertheless, the classic MBPC method generates a variable switching frequency, mainly due to the absence of a modulator. High frequency harmonics and higher stress on the power semiconductor devices are produced as a consequence of variable switching frequency [2]-[6]. To overcome these drawbacks, it is reported in the literature, a novel predictive control technique applied to a three-phase active rectifier [2], two-level voltage source inverters (VSI) [3]-[5], direct matrix converters (DMC) [6], [7], active power compensators [8], neutral pointed clamping (NPC) converters [9] and seven-level cascaded H-bridge back-to-back converter [10]. Of all of the different topologies and their applications, the cascaded H-bridge (CHB) multilevel converters-based is one of the most commonly used and an attractive topology due to their modularization, extensibility, control simplicity and high-quality output [11], [12]. The control simplicity in CHB multilevel converters, MBPC particularly, is mainly due to the finite number of possible states (including redundant states), however, intermediate states can not be computed and a bad references variables tracking is obtained, affecting the desired output waveforms.

In order to maintain the simplicity of MBPC applied to CHB multilevel converters and considering that the proposal presented in [2]-[10] has not been applied to multilevel static synchronous compensator (STATCOM) yet, this paper proposes extend this innovative predictive control strategy operating at fixed switching frequency to a single-phase CHB multilevel converter for STATCOM applications. The proposed approach predicts the future states of the system and generates the duty cycles for two active switching states and one null switching state which are applied to the single-phase CHB multilevel STATCOM using a given switching pattern. An optimization process considering a defined cost function allows calculating the duty cycles of each switching state.

II. Topology and Mathematical Model of the CHB STATCOM

The single-phase 7-level CHB converter-based STATCOM topology is shown in Fig. 1. Each H-bridge cell has four switching devices and an independent DC-link, being v_{dc} the voltage on the capacitor and C_{dc} the capacitance. To achieve the desired output voltage for each cell (v_i), four switching signals (s_{ij}) are needed, where i is the cell number and j the switching device (1, 2, 3 or 4). In order to avoid a short circuit in the DC-link, two switching signals and their complementary levels are used for each cell. As a result, there are $\varepsilon = 2^{2n_c}$ possible switching states for the desired output voltage of the STATCOM ($v_c = \sum_{i=1}^{n_c} v_i$), where n_c is the total number of cells. Moreover, each switching state is represented by a switching function ($F_s = \sum_{i=1}^{n_c} F_i$).

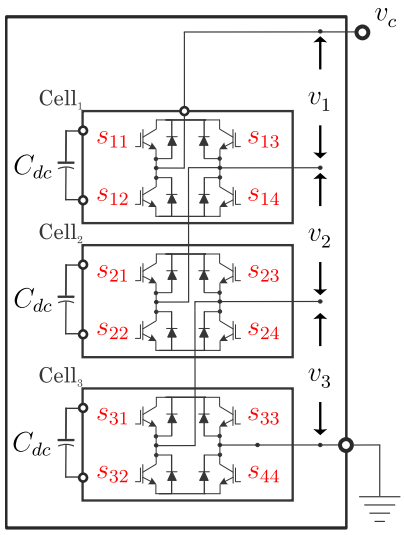

Fig. 1. Single-phase 7-level CHB converter-based STATCOM system.

Fig. 2 shows the load interconnected to one side to the CHB converter-based STATCOM system, and on the other side, to the electric power grid through the point of common coupling (PCC). Applying Kirchhoff's voltage law the dynamic model can be represented by the following equation:

$$\frac{\mathrm{d}i_c}{\mathrm{d}t} = \frac{v_s}{L_f} - \frac{R_f}{L_f} i_c - \frac{F_s v_{dc}}{L_f} \tag{1}$$

being L_f-R_f the inductor of the shunt power filter. The discrete time-domain model is obtained by using the forward Euler finite-difference approximation method:

$$i_c(k+1) = \left(1 - \frac{R_f T_s}{L_f}\right) i_c(k) + \frac{T_s}{L_f} \{v_s(k) - v_c(k)\} \tag{2}$$

where T_s is the sampling time, k identifies the actual discrete-time sample, and $i_c(k+1)$ is the prediction of the STATCOM current made at sample k.

III. Model Based Predictive Control Method

In the classic MBPC method for single-phase 7-level CHB multilevel STATCOM, Eq. (2) is used to calculate the prediction of the STATCOM current for each possible switching state ($F_{s,\eta}$, where η = 1, 2, ... or ε). Next, the predicted current error $ei_c(k+1)$ is computed by using the following equation:

$$ei_c(k+1) = i_c^*(k+1) - i_c(k+1) \tag{3}$$

being $i_c^*(k+1)$ the STATCOM current reference. Then, the quadratic measure of the predicted error is evaluated in a cost function typically defined as:

$$g(k+1) = \| \, ei_c(k+1) \, \|^2 \tag{4}$$

where $\| \ . \ \|$ denotes the magnitude of the variable. Finally, an optimization process selects, from all possible switching states (ε), the optimum switching state ($F_{s,opt}$) that generates

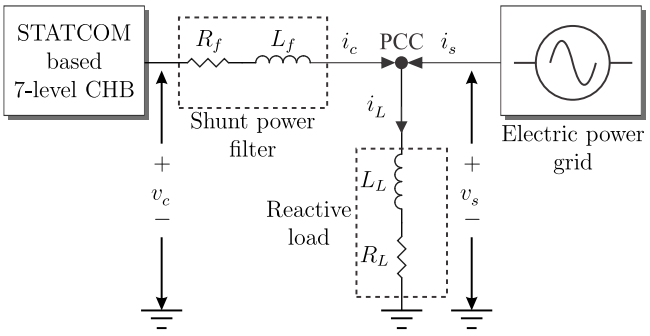

Fig. 2. STATCOM, load and electric grid connected through the PCC.

the minimum value of the defined cost function represented by (4) to apply in the next sampling time.

The block diagram of the classic MBPC method is shown in Fig. 3 (a) and Algorithm 1 summarizes the optimization process.

Algorithm 1 Optimization algorithm of the classic MBPC

1. Initialize $g_{opt} := \infty, \eta := 0$
2. Compute $i_c^*(k+1)$
3. **while** $\eta \leq \varepsilon$ **do**
4. Compute $i_c(k+1)$ for the η state
5. Compute $ei_c(k+1)$
6. Compute $g = g(k+1)$
7. **if** $g < g_{opt}$ **then**
8. $g_{opt} \leftarrow g, \quad F_{s,opt} \leftarrow F_{s,\eta}$
9. **end if**
10. $\eta := \eta + 1$
11. **end while**

IV. Proposed Predictive Control Strategy at Fixed Switching Frequency

The proposed predictive control strategy operating at fixed switching frequency predicts the future states of the system using Eq. (2) of all possible switching states, as the classic MBPC. However, in this case, is defined ϱ pairs of active switching states. The first pair (ξ = 1) consist in the first consecutive active switching states (η = 2 and η = 3, please refer to Appendix), the second pair (ξ = 2) consists in the last active switching state of the previous pair and the next consecutive active switching state (η = 3 and η = 5, please refer to Appendix), and so on. For each pair, three predictions are calculated (two active and one null). Next, a defined cost function represented by (4) is evaluated separately for each prediction. Then, with the calculated cost functions, duty cycles are calculated for each switching state. Finally, the three switching states and their respective duty cycles that generate the minimum value of a new cost function are applied using a given switching pattern in the next sampling time.

The block diagram of the proposed method is shown in Fig. 3 (b), where the switching pattern block is highlight.

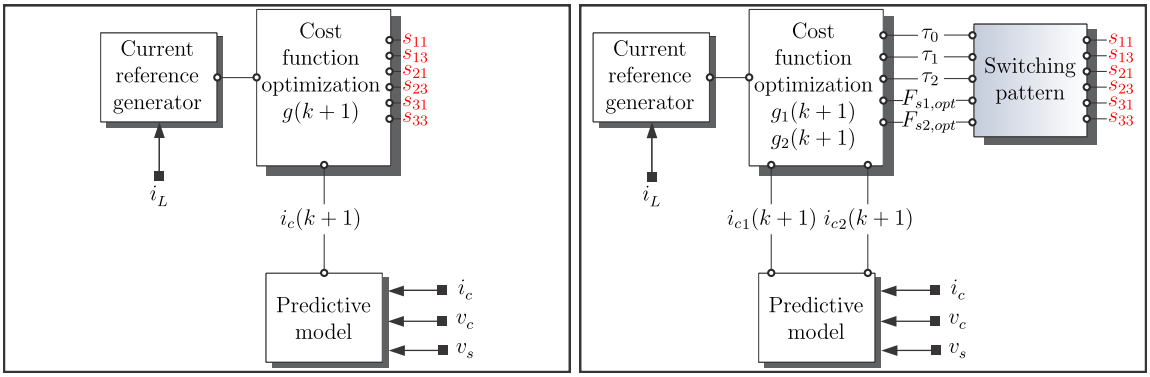

Fig. 3. Block diagram of (a) the classic MBPC and (b) the proposed MBPC at Fixed Switching Frequency.

A. Duty cycles calculation and switching pattern

The switching state that generates the lowest value of the cost function must be applied higher time, i.e., the duty cycle must be inversely proportional to the cost function. The duty cycles for the two active switching states and one null switching state are calculated by solving:

$$\begin{aligned} \tau_0 &= K/g_0 \\ \tau_1 &= K/g_1 \\ \tau_2 &= K/g_2 \\ \tau_0 + \tau_1 + \tau_2 &= 1 \end{aligned} \tag{5}$$

where τ_i are the duty cycles (0 correspond to the null switching state), g_i the cost functions represented by (4) and K is the constant of proportionality. Solving (5) for K, the expressions of the duty cycles for each switching state are given as:

$$\begin{aligned} \tau_0 &= g_1 g_2 / \left(g_0 g_1 + g_1 g_2 + g_0 g_2\right) \\ \tau_1 &= g_0 g_2 / \left(g_0 g_1 + g_1 g_2 + g_0 g_2\right) \\ \tau_2 &= g_0 g_1 / \left(g_0 g_1 + g_1 g_2 + g_0 g_2\right) \end{aligned} \tag{6}$$

With (6) is defined a new cost function as follows:

$$g = \tau_1 g_1 + \tau_2 g_2 \tag{7}$$

The switching pattern procedure is the one shown in Fig. 4 (where $T_i = \tau_i * T_s$). It is adopted with the goal of applying two active switching states and one null switching state, similar to [3],[4].

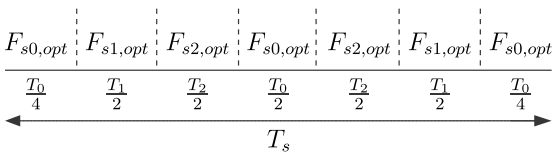

Fig. 4. Switching pattern for the optimal switching states.

B. Optimization process

The optimization process consist in to compute, the predictions, the cost functions and the duty cycles over all possible pairs of active switching states (ϱ). Since there are 44 active switching states (and 20 null) for the case study, the computation is performed $\varrho = 44$ times. To simplify the algorithm, only one null switching state ($\eta = 1$, please refer to Appendix) is used and it is calculated only one time. Algorithm 2 summarizes the optimization process.

Algorithm 2 Optimization algorithm of the proposed method

1. Initialize $g_{opt} := \infty, \xi := 0$
2. Compute $i_c^*(k+1)$
3. Compute $i_{c0}(k+1)$
4. Compute $ei_{c0}(k+1)$
5. Compute $g_0 = g_0(k+1)$
6. **while** $\xi \leq \varrho$ **do**
7. Compute $i_{c1}(k+1)$ and $i_{c2}(k+1)$
8. Compute $ei_{c1}(k+1)$ and $ei_{c2}(k+1)$
9. Compute $g_1 = g_1(k+1)$ and $g_2 = g_2(k+1)$
10. Compute τ_0, τ_1 and τ_2
11. Compute $g = \tau_1 g_1 + \tau_2 g_2$
12. **if** $g < g_{opt}$ **then**
13. $g_{opt} \leftarrow g$
14. Compute T_0, T_1 and T_2
15. $F_{s1,opt} \leftarrow F_{s1,\xi}, F_{s2,opt} \leftarrow F_{s2,\xi}$
9. **end if**
10. $\xi := \xi + 1$
11. **end while**

C. Reference generation

To allow an unitary power factor at the grid side, the instantaneous current reference can be written as:

$$i_c^*(k) = -i_{Lr}(k)\,\mathrm{sen}(\omega t + \frac{\pi}{2}) \tag{8}$$

being $i_{Lr}(k) = i_L(k)\,\mathrm{sen}(\theta)$ the reactive load current, $i_L(k)$ the load current measured at the instant k, θ the phase angle and ω the fundamental frequency.

The phase angle θ is obtained using a simple phase lock loop (PLL) closed-loop control system, provided by the development environment Matlab/Simulink.

V. Simulation Results

In order to validate the effectiveness of the proposed method, simulation results were carried out, considering the electrical parameters shown in Table I. The performance of the proposed MBPC are compared with the results obtained with the classical MBPC implementation, in both cases considering a sampling frequency of 25 kHz. The figure of merit used to compare quantitatively both controllers are the mean squared error (MSE) and the total harmonic distortion (THD). Equations (9) and (10) represent the parameters MSE and THD, respectively.

$$\text{MSE}(\Psi) = \sqrt{\frac{1}{N}\sum_{j=1}^{N}\Psi_j^2} \tag{9}$$

$$\text{THD} = \sqrt{\frac{1}{i_1^2}\sum_{i=2}^{N} i_i^2} \tag{10}$$

where Ψ is the tracking current error, N is the number of vector elements, i_1 is the amplitude of the fundamental frequency of the analyzed current, and i_i are the current harmonics.

TABLE I
Parameters Description

PARAMETER	SYMBOL	VALUE	UNIT
	Electric power grid		
Grid frequency	f_e	50	Hz
Grid voltage	v_s	310.2	V
	7-Level CHB STATCOM		
Filter resistance	R_f	0.09	Ω
Filter inductance	L_f	3	mH
DC-link voltage	v_{dc}	154	V
	Load parameters		
Load resistance	R_L	23.2	Ω
Load inductance	L_L	55	mH
	Predictive control parameters		
Sampling time	T_s	40	μs
Simulation step	–	1	μs

Fig. 5 show simulation results of the classical MBPC and the proposed control technique in Matlab/Simulink environment. A good current tracking and a fast dynamic response during the transient (after 0.02 s) is presented in Fig. 5 (bottom), having a reduction in the MSE from 0.5008 to 0.4254, compared with Fig. 5 (upper). Moreover, in Fig. 6 it is possible to notice how the mean reactive power is compensated, where $Q_c = -Q_L$ is the reactive power injected by the STATCOM and Q_s is the reactive power at the grid side.

A comparison analysis between the proposed method and the classical MBPC is shown in Fig. 7 considering; (upper) the switching pattern, (middle) the output voltages of the STATCOM and (bottom) the THD of the analyzed output voltage. As shown in Fig. 7 (b) a more sinusoidal output voltage v_c is obtained with respect to the output voltage than in Fig. 7 (a) due to the switching pattern procedure. Furthermore, the operation at fixed switching frequency produces a more concentrated spectrum, mainly around the switching frequency ($f_s = 25$ kHz).

Additionally, considering the interval 0.05 to 0.09 s, Fig. 8 shows the improvement obtained in the THD performance parameter of the grid current, that is about 47% (a drop from 8.29% to 4.37%) using the proposed method.

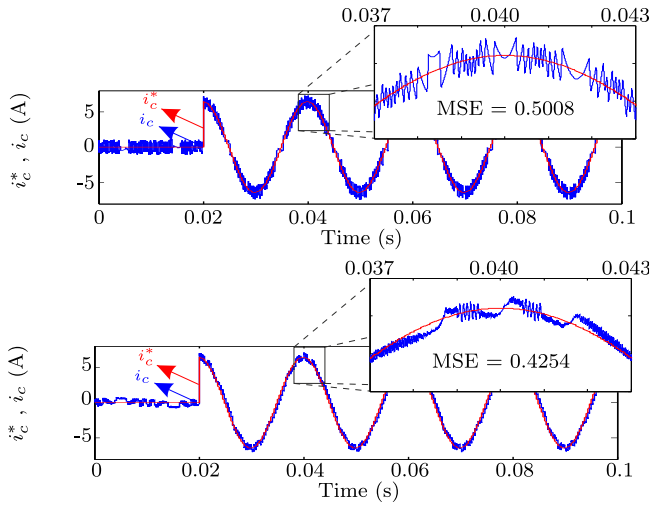

Fig. 5. Tracking current response: (upper) classical MBPC, (bottom) proposed MBPC.

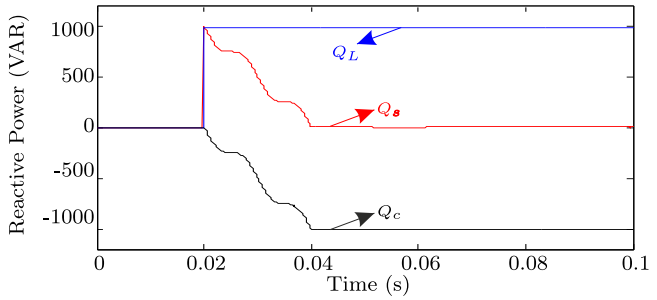

Fig. 6. CHB STATCOM steady-state and transient response with the proposed MBPC: (upper) tracking current, (bottom) reactive power compensation.

VI. Conclusion

In this paper, a MBPC operating at fixed switching frequency applied to the single-phase CHB 7-level STATCOM has been proposed. From the simulation results it is possible to confirm a good capability of the proposed control technique to compensate the reactive power and better performance in terms of THD and MSE, compared with the results obtained by the classical MBPC. A comparative simulation results performed with reference to the classical predictive control also show improvements relative to the output voltage.

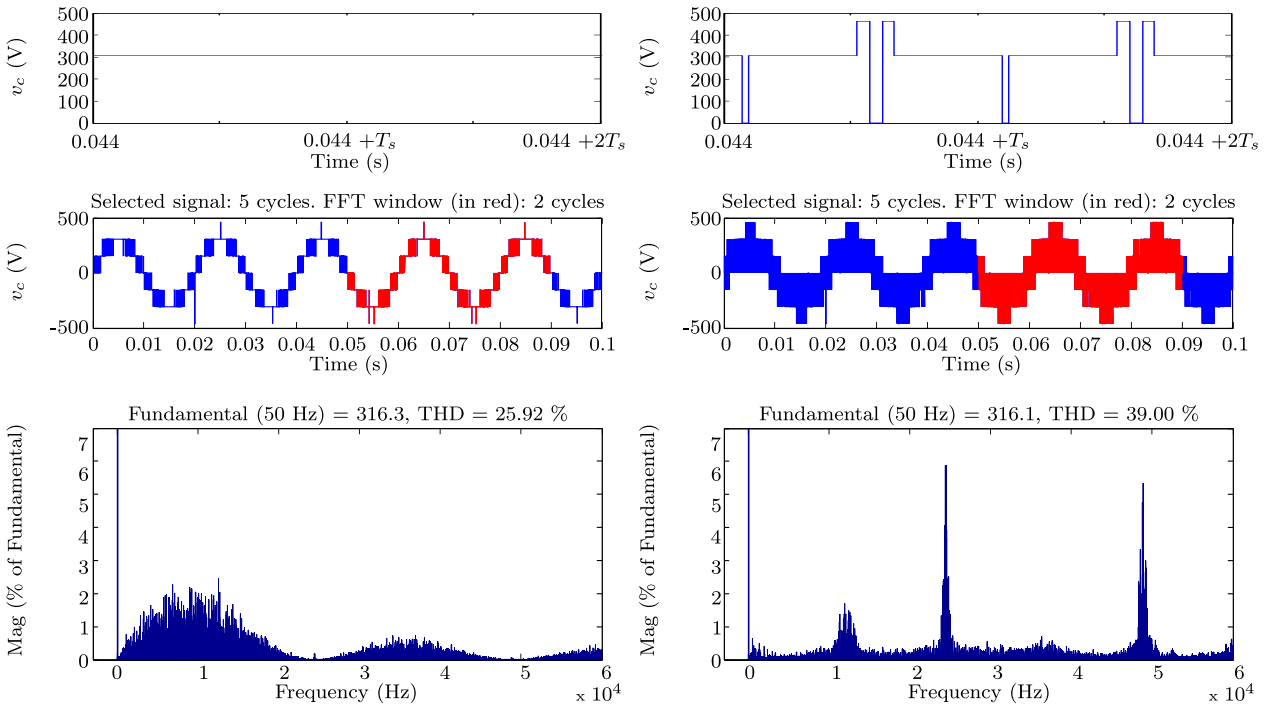

(a) Classical MBPC response

(b) Proposed MBPC with fixed switching frequency response

Fig. 7. Comparison performance considering: (upper) the switching pattern of the output voltage of the STATCOM obtained (middle) the output voltage of the STATCOM and (bottom) the THD of the output voltage.

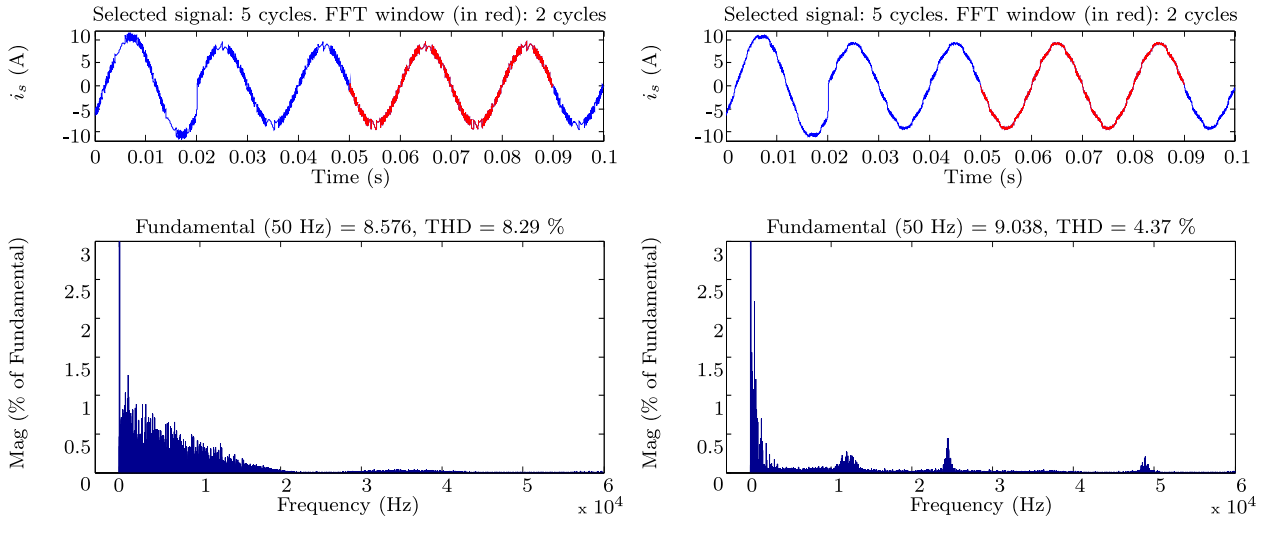

(a) Classical MBPC response

(b) Proposed MBPC with fixed switching frequency response

Fig. 8. Comparison performance considering: (upper) the grid current and (bottom) the THD of the grid current.

APPENDIX

TABLE II
SWITCHING FUNCTIONS FOR A SINGLE-PHASE 7-LEVEL CHB CONVERTER-BASED STATCOM SYSTEM

S_η						η	$F_{s,\eta}$
s_{11}	s_{13}	s_{21}	s_{23}	s_{31}	s_{33}		
0	0	0	0	0	0	1	0
0	0	0	0	0	1	2	-1
0	0	0	0	1	0	3	1
0	0	0	0	1	1	4	0
0	0	0	1	0	0	5	-1
0	0	0	1	0	1	6	-2
0	0	0	1	1	0	7	0
0	0	0	1	1	1	8	-1
0	0	1	0	0	0	9	1
0	0	1	0	0	1	10	0
0	0	1	0	1	0	11	2
0	0	1	0	1	1	12	1
0	0	1	1	0	0	13	0
0	0	1	1	0	1	14	-1
0	0	1	1	1	0	15	1
0	0	1	1	1	1	16	0
0	1	0	0	0	0	17	-1
0	1	0	0	0	1	18	-2
0	1	0	0	1	0	19	0
0	1	0	0	1	1	20	-1
0	1	0	1	0	0	21	-2
0	1	0	1	0	1	22	-3
0	1	0	1	1	0	23	-1
0	1	0	1	1	1	24	-2
0	1	1	0	0	0	25	0
0	1	1	0	0	1	26	-1
0	1	1	0	1	0	27	1
0	1	1	0	1	1	28	0
0	1	1	1	0	0	29	-1
0	1	1	1	0	1	30	-2
0	1	1	1	1	0	31	0
0	1	1	1	1	1	32	-1
1	0	0	0	0	0	33	1
1	0	0	0	0	1	34	0
1	0	0	0	1	0	35	2
1	0	0	0	1	1	36	1
1	0	0	1	0	0	37	0
1	0	0	1	0	1	38	-1
1	0	0	1	1	0	39	1
1	0	0	1	1	1	40	0
1	0	1	0	0	0	41	2
1	0	1	0	0	1	42	1
1	0	1	0	1	0	43	3
1	0	1	0	1	1	44	2
1	0	1	1	0	0	45	1
1	0	1	1	0	1	46	0
1	0	1	1	1	0	47	2
1	0	1	1	1	1	48	1
1	1	0	0	0	0	49	0
1	1	0	0	0	1	50	-1
1	1	0	0	1	0	51	1
1	1	0	0	1	1	52	0
1	1	0	1	0	0	53	-1
1	1	0	1	0	1	54	-2
1	1	0	1	1	0	55	0
1	1	0	1	1	1	56	-1
1	1	1	0	0	0	57	1
1	1	1	0	0	1	58	0
1	1	1	0	1	0	59	2
1	1	1	0	1	1	60	1
1	1	1	1	0	0	61	0
1	1	1	1	0	1	62	-1
1	1	1	1	1	0	63	1
1	1	1	1	1	1	64	0

ACKNOWLEDGMENT

The authors would like to thank to the Paraguayan Government for the economical support they provided through the CONACYT Grant 14-INV-096. This work was also made possible by the FONDECYT Regular Project N^{o} 1160690.

REFERENCES

[1] S. Kouro, M. A. Perez, J. Rodriguez, A. M. Llor, and H. A. Young, "Model predictive control: MPC's role in the evolution of power electronics," *IEEE Ind. Electron. Mag.*, vol. 9, DOI 10.1109/MIE.2015.2478920, no. 4, pp. 8–21, Dec 2015.

[2] L. Tarisciotti, P. Zanchetta, A. Watson, J. C. Clare, M. Degano, and S. Bifaretti, "Modulated model predictive control for a three-phase active rectifier," *IEEE Trans. Ind. Electron.*, vol. 51, no. 2, pp. 1610–1620, Mar 2015.

[3] M. Rivera, F. Morales, C. Baier, J. Muoz, L. Tarisciotti, P. Zanchetta, and P. Wheeler, "A modulated model predictive control scheme for a two-level voltage source inverter," in *Proc. ICIT*, Mar 2015, pp. 2224–2229.

[4] M. Rivera, "A new predictive control scheme for a vsi with reduced common mode voltage operating at fixed switching frequency," in *Proc. POWERENG*, May 2015, pp. 617–622.

[5] M. Tomlinson, T. Mouton, and R. Kennel, "Finite-control-set model predictive control with a fixed switching frequency vs. linear control for current control of a single-leg inverter," in *Proc. PRECEDE*, Oct 2015, pp. 109–114.

[6] M. Vijayagopal, P. Zanchetta, L. Empringham, L. D. Lillo, L. Tarisciotti, and P. Wheeler, "Modulated model predictive current control for direct matrix converter with fixed switching frequency," in *Proc. EPE'15 ECCE*, Sept 2015, pp. 1–10.

[7] M. Vijayagopal, L. Empringham, L. de Lillo, L. Tarisciotti, P. Zanchetta, and P. Wheeler, "Current control and reactive power minimization of a direct matrix converter induction motor drive with modulated model predictive control," in *Proc. PRECEDE*, Oct 2015, pp. 103–108.

[8] R. Rabbeni, L. Tarisciotti, A. Gaeta, A. Formentini, P. Zanchetta, M. Pucci, M. Degano, and M. Rivera, "Finite states modulated model predictive control for active power filtering systems," in *Proc. ECCE*, Sept 2015, pp. 1556–1562.

[9] M. Norambuena, H. Yin, S. Dieckerhoff, and J. Rodriguez, "Improved finite control set model predictive control with fixed switching frequency for three phase npc converter," in *PCIM*, May 2016, pp. 1–8.

[10] L. Tarisciotti, P. Zanchetta, A. Watson, S. Bifaretti, and J. C. Clare, "Modulated model predictive control for a seven-level cascaded h-bridge back-to-back converter," *IEEE Trans. Ind. Electron.*, vol. 61, no. 10, pp. 5375–5383, Oct 2014.

[11] R. Gregor, A. Renault, L. Comparatore, J. Pacher, J. Rodas, D. Gregor, J. Muñoz, and M. Rivera, "Finite-states model predictive control with increased prediction horizon for a 7-level cascade h-bridge multilevel STATCOM," in *Proc. WMSCI*, Jul 2016.

[12] R. Gregor, L. Comparatore, A. Renault, J. Rodas, J. Pacher, S. Toledo, and M. Rivera, "A novel predictive-fixed switching frequency technique for a cascade H-Bridge multilevel STATCOM," in *Proc. IECON*, Oct 2016.